

考虑两相流音速时气固两相流激波研究

赵良举, 高丽娟, 袁悦祥, 曾丹苓
(重庆大学 动力工程学院, 重庆 400044)

摘 要: 建立了基于两相流音速的气固两相流激波模型, 并进行了计算分析。与基于单相流音速的激波模型的计算结果比较发现, 当气相体积比较大时, 两种模型所计算的音速差别较小, 激波的结果是吻合的; 当气相体积比较小时, 两相音速模型所计算的音速值与实际值更接近, 其激波结果更合理。因此本文基于两相流音速模型的激波分析更具通用性。

关 键 词: 气固两相流; 音速; 激波

中图分类号: O359 文献标识码: A

1 引 言

超音速冷喷涂(CSC), 又称为冷空气动力学喷涂(CGDS), 是一种新型的喷涂表面沉积的方法^[1-3]。在超音速冷喷涂中, 喷涂粉末与气体混合后, 在缩放流道内形成超音速流动, 与基板碰撞后喷涂粒子在基板上沉积。由于两相介质是超音速流动, 此时气固两相流激波起着至关重要的作用。

气固两相流激波远远复杂于单相流激波, 首先表现在两相流的音速变化^[4], 粒子的大小、相间滑移和相间热交换强弱, 都会对其产生影响^[5]。关于气固两相流激波研究的报导很少, 仅见文献[6]。Jackson 等人以单相流音速对两相流激波进行了研究^[6]。由于没有考虑两相流音速随两相体积比的变化, 因而适用于固相比例较小时的两相流激波分析。

本文将在 Jackson 等人的研究基础上, 引入两相流音速的计算, 对气固两相流激波进行研究。计算分析结果显示, 在固相体积比较小时, 文献[6]的单相流模型的结果与本文的两相流模型结果吻合, 当固相体积比较大时, 两相流模型结果较单相流模型的结果合理, 因而更具通用性。

2 气固两相音速的计算

关于音速的研究较多, 主要集中在汽液两相介质音速的分析。如曾丹苓、陈听宽和刘大有等人对两相流音速有深入的研究^[7-9]。然而对气固两相介质音速研究者较少。普朗特关于气固两相介质音速的定性分析认为^[4], 对于空气中的雪或沙, 由于具有空气的压缩作用, 密度却比空气大得多, 因而音速将远小于单相音速。曾丹苓研究发现^[7], 影响音速的因素较多, 如空泡率、相变、相间热交换和粘性摩擦等, 但音速的主要影响因素是空泡率和相变。对于气固两相介质没有相变发生, 忽略不可逆因素的影响, 本文将从定熵音速公式出发, 推导并计算气固两相流的音速随固相体积比的变化。

由 Laplace 定熵音速公式:

$$a_s = \sqrt{\left(\frac{\partial p}{\partial \rho}\right)_s} \quad (1)$$

经推导可得:

$$a = v \left[- \left[(v_g - v_p) \left(\frac{\partial(1-x)}{\partial \rho} \right)_s + (1-x) \frac{dv_g}{dp} + x \frac{dv_p}{dp} \right] \right]^{-1/2} \quad (2)$$

式中: v —比容; h —焓; p —压力; x —固相质量比。下标: g, p —气相与固相。固相体积比 α , 满足 $x = \alpha \rho_p / [\alpha \rho_p + (1-\alpha) \rho_g]$, ρ 为密度。由 $h = (1-x)h_g + xh_p$ 可知:

$$x = \frac{h - h_g}{h_p - h_g} \quad (3)$$

代入式(2), 得:

$$a = v \left[- \left[(v_g - v_p) \left(\frac{dh/dp}{h_g - h_p} \frac{(h_g - h)dh_p/dp + (h - h_p)dh_g/dp}{(h_g - h_p)^2} \right)_s + (1-x) \frac{dv_g}{dp} + x \frac{dv_p}{dp} \right] \right]^{-1/2} \quad (4)$$

将空气视为理想气体, 有 $p_g v_g = R_g T$, 固相的焓和比容与压力无关, 有 $dh_p/dp = 0, dv_p/dp = 0$, 上式简化为:

$$a = v \left[- (v_g - v_p) \frac{c_{pg} v_g}{R_g} \left(1 - \frac{1}{k_g} \right) \right] \times$$

$$\left(\frac{1-x}{h_g-h_p} - \frac{(h-h_p)}{(h_g-h_p)^2} \right) + \frac{(1-x)v_g}{kp} \Big)^{-1/2} \quad (5)$$

式中: c_{pg} —气相定相比热; k_g —气相比热比。

以空气和干沙的气固两相流为例的计算结果如图 1 和图 2 所示。计算结果表明, 当气相体积比为 10%~95% 时, 气固两相流的音速大大低于空气中的音速。当气相体积比为 50% 时, 音速最低值约为 20 m/s。当气相体积比很小时, 两相流音速接近固相音速, 当气相体积比接近于 1 时, 两相流音速接近气相音速。此结果与普朗特的分析是吻合的, 与气液两相流的音速结果也是类似的^[7]。同时, 从图 1 可知, 压力增加时音速有小幅增加。温度对气固两相流音速的影响在低气相体积比很小, 气相比例增加温度影响增大, 气相体积比接近 100% 时, 温度影响明显, 如图 2 所示。

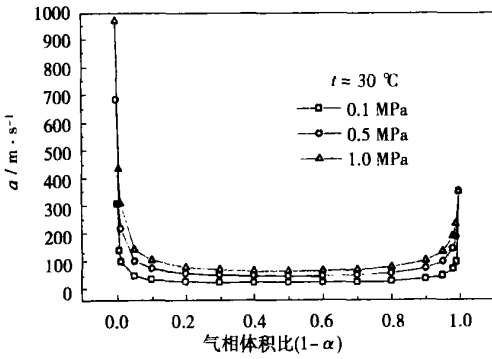


图 1 不同压力下的气固两相流音速

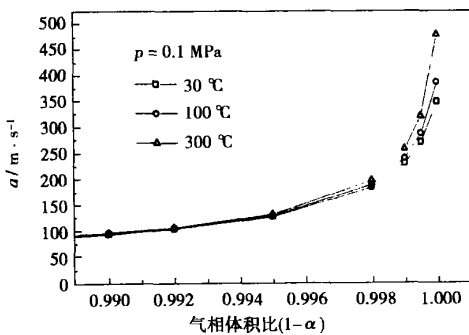


图 2 不同温度下的气固两相流音速

3 气固两相流激波数学模型的建立

Jackson 等人对气固两相流激波进行了分析计算^[9], 用单相气相音速作为两相音速进行分析, 当固相很少时, 两相流体音速可近似认为与气相音速相同, 采用单相音速模型定义的马赫数与实际马赫数接近。但当固相比例较大时, 采用单相音速模型定

义的马赫数与实际马赫数相差较大。因此本文考虑了气固两相流音速, 用两相流音速代替单相音速, 对气固两相流激波进行分析。

数学模型为质量守恒方程、动量方程和能量守恒方程。用 x 表示固相与总质量之比, σ 表示两相速度转移系数, m 表示质量流量, u 表示速度; 用下标 p、g 分别代表固相和气相, a、b 代表波后和波前参数, 则有:

$$x = \frac{m_p}{m_p + m_g} \quad (6)$$

$$\sigma = u_p / u_g \quad (7)$$

由质量守恒:

$$\rho_{g,b} u_{g,b} = \rho_{g,a} u_{g,a} \quad (8)$$

定义无量纲参数:

$$\tilde{u} = u / u_{g,b} \quad (9)$$

$$T = T / T_{g,b} \quad (10)$$

$$\tilde{p} = p / p_{g,b} \quad (11)$$

$$\rho = \rho / \rho_{g,b} \quad (12)$$

式(8)无量纲化为:

$$\rho_{g,a} \tilde{u}_{g,a} = 1 \quad (13)$$

气相在波前和波后满足理想气体状态方程:

$p_g = \rho_g R_g T_g$, 此式可写为如下无量纲形式:

$$P_{g,a} = \rho_{g,a} T_{g,a} \quad (14)$$

由动量方程可得:

$$(p_b - p_a) A = (u_{g,a} - u_{g,b}) \rho_{g,b} u_{g,b} A + (u_{p,a} - u_{p,b}) \rho_{p,b} u_{p,b} A \quad (15)$$

由式(6)有:

$$x = \frac{m_p}{m_p + m_g} = \frac{\rho_{p,b} u_{p,b}}{\rho_{p,b} u_{p,b} + \rho_{g,b} u_{g,b}} \quad (16)$$

移项并简化得:

$$\rho_{p,b} = \rho_{p,b} \frac{x}{\sigma_b (1-x)} \quad (17)$$

将上式代入式(15)有:

$$p_b - p_a = (u_{g,a} - u_{g,b}) \rho_{g,b} u_{g,b} + (\sigma_a u_{g,a} - \sigma_b u_{g,b}) \rho_{g,b} u_{g,b} \frac{x}{1-x} \quad (18)$$

将上式两边分别除以 $\rho_{g,b} u_{g,b}^2$ 得:

$$\frac{p_b}{\rho_{g,b} u_{g,b}^2} - \frac{p_a}{\rho_{g,b} u_{g,b}^2} = \left(\frac{u_{g,a}}{u_{g,b}} - 1 \right) + \left(\sigma_a \frac{u_{g,a}}{u_{g,b}} - \sigma_b \right) \times \frac{x}{1-x} \quad (19)$$

考虑两相流音速与单相流音速的差别, 令 η_i 为两相流音速与气相音速的比值:

$$\eta_i = a_i / a_{g,i} \quad (20)$$

其中: a_i —两相流音速; $a_{g,i}$ —气相音速, i 取值为 a 和 b , 分别代表波后和波前。用两相流音速来计算马赫数 Ma , 波前马赫数可表示为:

$$M_{g,b} = \frac{u_{g,b}}{a_b} = \frac{u_{g,b}}{a_{g,b} \eta_b} \quad (21)$$

将上式代入式(19)并整理有:

$$\frac{1}{M_{g,b}^2 \eta_b \gamma_g} + (1 + \sigma_b \frac{x}{1-x}) = P_{g,a} \frac{1}{M_{g,b}^2 \eta_b \gamma_g} + (1 + \sigma_a \frac{x}{1-x}) \tilde{u}_{g,a} \quad (22)$$

同时, 波前、波后应满足能量守恒方程:

$$m_g (c_{p,g} T_{g,b} + \frac{u_{g,b}^2}{2}) + m_p (c_{v,p} T_{p,b} + \frac{u_{p,b}^2}{2} + p_b v_{p,b}) = m_g (c_{p,g} T_{g,a} + \frac{u_{g,a}^2}{2}) + m_p (c_{v,p} T_{p,a} + \frac{u_{p,a}^2}{2} + p_a v_{p,a}) \quad (23)$$

对稀疏两相流, 忽略固相体积, 并引入滑移系数有:

$$(1-x)(c_{p,g} T_{g,b} + \frac{u_{g,b}^2}{2}) + x(c_{v,p} T_{p,b} + \sigma_b^2 \frac{u_{g,b}^2}{2}) = (1-x)(c_{p,g} T_{g,a} + \frac{u_{g,a}^2}{2}) + x(c_{v,p} T_{p,a} + \sigma_b^2 \frac{u_{g,a}^2}{2}) \quad (24)$$

对固相, 可认为 $C_{v,p} = C_{p,p}$, 并定义以下无量纲两相温度比:

$$H_i = T_{p,i} / T_{g,i} \quad (25)$$

式(24)可写为:

$$(1-x)(c_{p,g} T_{g,b} + \frac{u_{g,b}^2}{2}) + x(c_{p,p} H_b T_{g,b} + \sigma_b^2 \frac{u_{g,b}^2}{2}) = (1-x)(c_{p,g} T_{g,a} + \frac{u_{g,a}^2}{2}) + x(c_{p,p} H_a T_{g,a} + \sigma_a^2 \frac{u_{g,a}^2}{2}) \quad (26)$$

将气相音速表达式 $a_{g,b} = \sqrt{k_g R_g T_{g,b}}$ 代入式(21)可得 $T_{g,b}$:

$$T_{g,b} = \frac{u_{g,b}^2}{M_{g,b}^2 \eta_b \kappa_g R_g} \quad (27)$$

同时, 定义固相与气相的比热比 C_r 为: $C_r = c_{p,p} / c_{p,g}$, 对理想气体有:

$$\frac{C_{p,g}}{R_g} = \frac{\kappa_g}{\kappa_g - 1} \quad (28)$$

其中: $\kappa_g = c_{p,g} / c_{v,g}$ 。

式(26)两端同时除以 $(R_g T_{g,b})$, 可表示为:

$$(1-x) \left[\frac{\kappa_g}{\kappa_g - 1} + \frac{M_{g,b}^2 \eta_b \kappa_g}{2} \right] + x \left[\frac{C_r H_b \kappa_g}{\kappa_g - 1} + \frac{\sigma_b^2 M_{g,b}^2 \eta_b \kappa_g}{2} \right] = (1-x) \times$$

$$\left[\frac{\kappa_g}{\kappa_g - 1} \frac{T_{g,a}}{T_{g,b}} + \frac{M_{g,b}^2 \eta_b \kappa_g}{2} \left(\frac{u_{g,a}}{u_{g,b}} \right)^2 \right] + x \left[\frac{C_r H_a \kappa_g}{\kappa_g - 1} \frac{T_{g,a}}{T_{g,b}} + \frac{\sigma_a^2 M_{g,b}^2 \eta_b \kappa_g}{2} \left(\frac{u_{g,a}}{u_{g,b}} \right)^2 \right] \quad (29)$$

引入无量纲参数, 有:

$$(1-x) \left[\frac{\kappa_g}{\kappa_g - 1} + \frac{M_{g,b}^2 \eta_b \kappa_g}{2} \right] + x \left[\frac{C_r H_b \kappa_g}{\kappa_g - 1} + \frac{\sigma_b^2 M_{g,b}^2 \eta_b \kappa_g}{2} \right] = (1-x) \times \left[\frac{\kappa_g}{\kappa_g - 1} \frac{T_{g,a}}{T_{g,b}} + M_{g,b}^2 \eta_b \kappa_g \frac{\tilde{u}_{g,a}^2}{2} \right] + x \left[\frac{C_r H_a \kappa_g}{\kappa_g - 1} \frac{T_{g,a}}{T_{g,b}} + \sigma_a^2 M_{g,b}^2 \eta_b \kappa_g \frac{\tilde{u}_{g,a}^2}{2} \right] \quad (30)$$

波后马赫数可以表示为:

$$M_{g,a} = \frac{u_{g,a}}{a_a} = \frac{\tilde{u}_{g,a} u_{g,b}}{\sqrt{\kappa_g R_g T_{g,a} T_{g,b}} \eta_a} = \frac{\tilde{u}_{g,a}}{\sqrt{T_{g,a}}} \frac{\eta_b}{\eta_a} M_{g,b} \quad (31)$$

联立求解式(13)、式(14)、式(22)、式(30)和式(31), 可得波后无量纲参数 $\tilde{p}_{g,a}$ 、 $\tilde{p}_{g,b}$ 、 $\tilde{u}_{g,a}$ 、 $T_{g,a}$ 和 $M_{g,b}$ 的解。

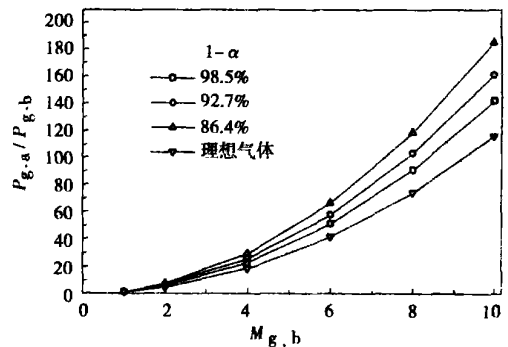


图 3 激波升压比与波前马赫数的关系

4 气固两相流激波计算结果分析

为了分析气相体积比对激波的影响, 不考虑相间滑移和相间热交换影响, 两相速度滑移系数和无量纲两相温度比均取值为 1, 即 $\sigma_a = \sigma_b = 1.0$ $H_a = H_b = 1.0$, 波前温度为 30°C , 压力为 0.1 MPa 。对空气与干沙的两相流激波计算结果与理想气体激波进行了比较, 如图 3~6 所示。从图 3 中可以看出, 对相同的波前马赫数, 两相流激波的升压比较单相理想气体高, 气相体积比越低, 激波升压比越高。如图 4~6 所示, 对相同的波前马赫数, 两相流激波的波后无量纲速度、波后马赫数和无量纲温度较单相流低。

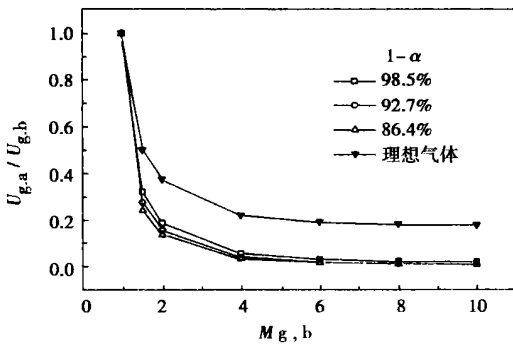


图 4 波后无量纲速度与波前马赫数的关系

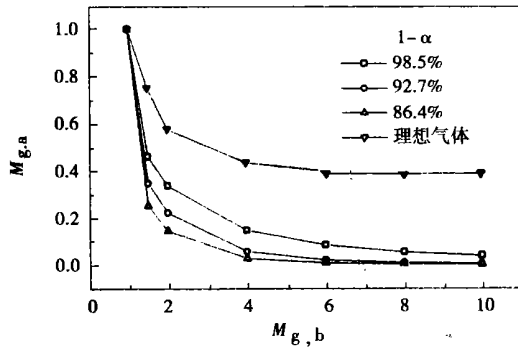


图 5 波后马赫数与波前马赫数的关系

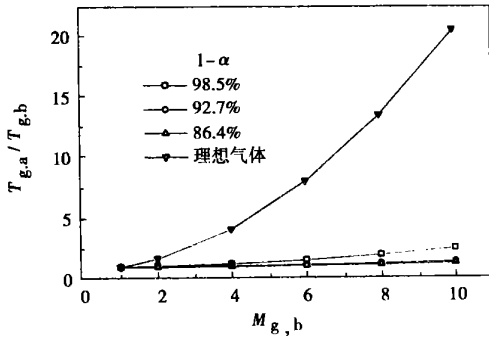


图 6 波后无量纲温度与波前马赫数的关系

5 单相音速和两相音速模型激波结果的比较

本文将两相流模型的激波结果与 Jackson 的单相音速模型的激波结果进行了比较, 不考虑速度滑移和相间热交换的影响, 针对常温常压下的气固两相流激波进行分析。波前温度为 30 °C, 压力为 0.1 MPa, 气固两相流激波的比较分析结果如图 7 和图 8 所示。当气相体积比 (99.99%) 较大时, 固相占的比例很小, 此时单相空气的音速为 348.73 m/s, 两相流

音速值为 330.86 m/s, 两种音速值的差别很小, 从图 7 可知两种模型的结果是吻合的。当气相体积比 (92.7%) 较小时, 两相流体的音速值差别变大, 此时单相空气的音速为 348.73 m/s, 两相流音速值为 37.52 m/s, 两种模型得出的气固两相流激波的结果差别相当大如图 8 所示是两种模型的激波与理想气体激波的比较, 此时按两相音速模型所得的结果与理想气体的结果吻合, Jackson 按单相音速模型所得激波, 在马赫数较小时, 得到了相当高的波后升压比, 如 $M_{g,b} = 4$, $p_{g,a} / p_{g,b} = 2\ 235$, 这与实际情况相差很大, 正是由于音速计算的较大差别使激波计算结果出现了较大偏差。

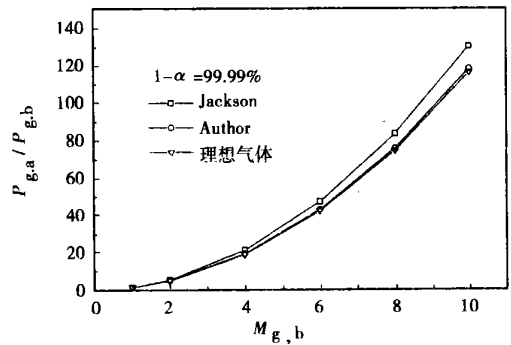


图 7 高气相体积比时两种模型的激波比较

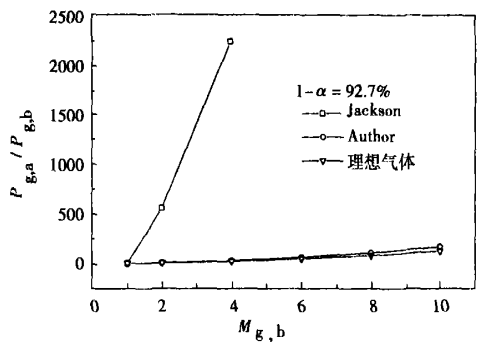


图 8 较低气相体积比时两种模型的激波比较

从以上分析可得, 对气固两相流激波的分析, 在气相体积比较大时, Jackson 模型与本文模型的结果是吻合的, 而气相体积比较小时, 两种模型的差别变大, 本文模型由于考虑了两相音速的变化, 激波结果更合理, 适用性更广。

6 结论

(下转第 69 页)

为了综合衡量分散度, 引入平均径跨 \overline{SPAN} 的概念, 即用流量加权平均数表示 \overline{SPAN} :

$$\overline{SPAN} = \frac{\sum_i Q_i (SPAN)_i}{\sum_i Q_i} \quad (3)$$

几何相似各喷嘴的平均径跨 \overline{SPAN} 整理如图 11 所示。

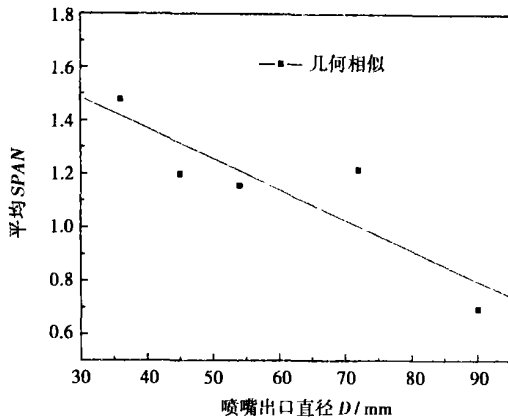


图 11 平均径跨随出口直径变化曲线图

由图可以看出, 几何相似喷嘴随出口直径的增加平均径跨 \overline{SPAN} 减小, 分散度减小, 雾化质量提高。这是由于进出口直径大, 液体在旋流腔的旋转时间长, 流动稳定性好, 液膜形成较均匀, 出流散裂较好。可见喷嘴结构参数对粒径分布均匀性影响较大。

5 结 论

通过对空心锥偏心旋流喷嘴的试验研究可以得到如下结论:

(1) 旋流喷嘴结构参数对雾化特性的影响较大, 可以通过改变其结构优化雾化特性。

(2) 旋流喷嘴体积流量与压力的平方根成线性关系。在几何相似时, 流量随压力的变化遵循相似规律; 在仅喷孔直径变化时, 随孔径的增加流量压力曲线斜率增加。为保证此种喷嘴运行经济性, 进出口直径应控制在一定范围内。

(3) 雾化粒径随压力增加而减小, 高压时压力对改变粒径的作用不明显; 在出口直径约 60 mm 时, 雾化粒径对压力的变化最敏感。仅喷孔直径变化时, 随着喷孔直径的减小, 旋流喷嘴雾化粒径对压力的敏感度降低。雾化粒径随流量先减小后增大。

(4) 雾化角随压力的变化不明显。相同压力下, 仅出口直径变化时雾化角基本不变。

(5) 采用径跨来分析雾化粒度分布, 得到如下规律: 随着出口直径的增加平均径跨 \overline{SPAN} 减小, 分散度减小, 雾化质量提高, 即大口径旋流喷嘴的雾化质量较好。

参考文献:

- [1] 郝吉明, 马广大. 大气污染控制工程[M]. 第二版. 北京: 高等教育出版社, 2002.
- [2] 马斯托思 K. 喷雾干燥手册[M]. 黄照柏, 冯尔健, 译. 北京: 中国建筑工业出版社, 1983.
- [3] 岑可法, 姚强, 曹欣玉, 等. 煤浆燃烧、流动、传热和气化的理论与应用技术[M]. 杭州: 浙江大学出版社, 1997.
- [4] 谢明湖. 高粘度液体液料 Y 型喷嘴的雾化机理及其雾化性能研究[J]. 工程热物理学报, 1992, 13(4): 425-430.

(何静芳 编辑)

(上接第 65 页)

本文对气固两相流音速与激波进行了分析计算, 并与 Jackson 模型作了对比, 得到以下结论:

(1) 气固两相流音速比单相的音速低的多, 在气相体积比为 50% 附近出现最小值;

(2) 采用两相音速模型分析两相流激波, 比用单相音速模型所得的结果更合理, 适用性更广。

参考文献:

- [1] ALKIMOV A P, KOSAREV V F, POPYRIN A N. A method of cold gas dynamic deposition[J]. Dokl Akad Nauk SSSR 1990 315(5): 1062-1065.
- [2] VAN STEENKISTE T H, SMITH J R, TEETS R E, et al. Kinetic spray coatings[J]. Surface and Coatings Technology, 1999 111: 62-71.
- [3] VAN STEENKISTE T H, SMITH J R, TEETS R E. Aluminum coatings

via kinetic spray with relatively large powder particles[J]. Surface and Coatings Technology, 2002, 154: 237-252.

- [4] 普朗特 L. 流体力学概论[M]. 北京: 科学出版社, 1984.
- [5] 赵良举. 非平衡两相热流体的流动、激波及其应用研究[D]. 重庆: 重庆大学, 2001.
- [6] JACKSON C R, LEAR W E, SHERIF S A. Generalized wave analysis of two-phase flow[J]. Mechanics Research Communications, 1998, 25(6): 613-622.
- [7] ZENG DANLING, ZHAO LIANGJU. Sound velocity in vapor-liquid two-phase fluid system[A]. Proceedings of ICECA[C]. Wuhan: Huazhong University of Science and Technology Press 2001. 50-55.
- [8] 徐进良, 陈听宽. 汽液两相流中的声速研究[J]. 西安交通大学学报, 1994, 28(5): 73-81.
- [9] 刘大有. 两相速度平衡条件下的两相流声速[J]. 力学学报, 1990 22(6): 660-669.

(何静芳 编辑)

Key words: natural gas, small-scale combustion, combustion characteristics, heat conduction

飞灰回燃对燃烧福建无烟煤 CFB 锅炉运行影响的研究 = **An Investigation of the Impact of Fly-ash Reburning on the Operation of an Anthracite-firing CFB (Circulating Fluidized Bed) Boiler** [刊, 汉] / HE Hong-zhou (Institute of Energy and Power Engineering under the Jimei University, Xiamen, China, Post Code: 361021) // Journal of Engineering for Thermal Energy & Power. — 2006, 21(1). — 53 ~ 57

The reactivity of fly-ash carbon and that of other coals fed into a boiler was investigated and compared through experiments with the help of a thermobalance. A theoretical analysis was conducted of the impact of fly-ash reburning on the combustion efficiency of a CFB (circulating fluidized bed) boiler. Moreover, by way of industrial tests investigated and measured was the impact of the fly-ash quantity recycled for reburning on the following items: the operating temperature of a recycle-to-boiler device, fly-ash particle distribution and its carbon content, boiler combustion efficiency and other operating parameters. The results of the investigation indicate that the reactivity of fly-ash carbon of the CFB boiler burning Fujian anthracite is higher than that of other corresponding coals fed into the boiler. In addition, other parameters, such as carbon content of the reburnt fly ash, the ratio of the reburnt fly ash amount to other coals fed into the boiler, have a major influence on the combustion efficiency of the boiler. The use of fly-ash reburning technology will be conducive to reducing the carbon content of the fly ash and the operating temperature of recycle-for reburning device as well as enhancing the combustion efficiency of the boiler. However, a relatively large amount of fly ash assigned for reburning will affect the stable operation of the boiler. **Key words:** Fujian anthracite, circulating fluidized bed boiler, fly ash, reburning

燃煤飞灰伏安特性的实验研究 = **Experimental Study of the Volt-ampere Characteristics of Fly Ash Resulting from Coal Firing** [刊, 汉] / YUAN Yong-tao, QI Li-qiang (Institute of Environmental Science & Engineering under the North China University of Electric Power, Baoding, China, Post Code: 071003) // Journal of Engineering for Thermal Energy & Power. — 2006, 21(1). — 58 ~ 61

The dielectric character of fly ash is a major factor having an impact on the efficiency of electrostatic precipitators. By employing a self-developed direct-current high voltage test system the current leakage and specific resistance of the fly ash of various kinds of coal being fired were measured and analyzed, and a series of volt-ampere characteristic curves obtained. It has been found that the relation among the following three items, i. e., the voltage applied to the ash layer, the current leakage through the ash layer and fly-ash specific resistance, does not always conform to the classic Ohm's law, namely, $V/I \neq \text{constant}$. At the three segments of high, middle and low voltage the volt-ampere characteristic curves of the fly ash have different configuration features. With an increase in voltage the specific resistance of the fly ash assumes a descending tendency with the range of descending amount being within one order of magnitude ($10^1 \Omega \cdot \text{cm}$). The cause leading to the occurrence of this phenomenon consists in the high-resistance feature of the fly ash. Meanwhile, this is also closely related with the physical-chemical properties of the coal rank and fly ash. **Key words:** fly ash of coal fired, dielectric properties, specific resistance, electrostatic precipitator

考虑两相流音速时气固两相流激波研究 = **A Study of Two-phase Shock Waves with a Two-phase Flow Sonic Velocity being Taken into Account** [刊, 汉] / ZHAO Liang-ju, GAO Li-juan, YUAN Yue-xiang, et al (Institute of Power Engineering under the Chongqing University, Chongqing, China, Post Code: 400044) // Journal of Engineering for Thermal Energy & Power. — 2006, 21(1). — 62 ~ 65, 69

On the basis of a two-phase flow sonic velocity a gas-solid two-phase flow shock-wave model was set up, and calculations and analyses were performed. When compared with the calculation results of a shock wave model based on a single-phase flow sonic velocity it has been found that in the case of a relatively large gas-phase volume the sonic velocity difference as calculated by using the above two kinds of models is relatively small and the shock wave results for the two models are in good agreement. When the gas phase volume is relatively small, the sonic velocity value calculated through the use of the two-phase sonic velocity model is in better correspondence with the actual value, resulting in more rational shock wave re-

sults. In view of the above, the shock wave analysis based on the two-phase flow sonic velocity model is more suited for general applications. **Key words:** gas-solid two phase flow, sonic velocity, shock wave

湿法烟气脱硫旋流喷嘴雾化特性研究 = **A Study of the Atomization Characteristics of Swirl Spray Nozzles Used in a Wet-process Flue-gas Desulfurization Unit** [刊, 汉] / LI Zhao-dong, WANG Shi-he (Department of Municipal Construction Engineering, Southeastern University, Nanjing, China, Post Code: 210096), WANG Xiao-ming (Guodian Environmental Protection Research Institute, Nanjing, China, Post Code: 210031) // Journal of Engineering for Thermal Energy & Power. — 2006, 21(1). — 66 ~ 69

Atomization spray nozzles are key components in a wet-process flue-gas desulfurization sprinkling tower. The quality of atomization can directly affect desulfurization efficiency and the utilization rate of a desulfurization agent. Tests were conducted with the hollow cone-shaped and eccentric swirl nozzle often used in wet-process flue-gas desulfurization technology serving as an object of investigation. Developed were a series of geometrically similar spray nozzles and also those with a change only in outlet diameters. A systematic study was performed of the above-mentioned nozzle as regards the following characteristics: volumetric flow rate, atomization particle diameter, atomization angle, and atomization particle distribution, etc. From the tests a set of rules or laws governing the following factors were obtained: the variation of volumetric flow rate with a change in pressure and spray nozzle structure, the variation of atomization particle diameter with a change in pressure, flow rate and spray nozzle structure, the variation of atomization angle with a change in pressure, etc. Average-diameter span was used to indicate the dispersion degree for judging the distribution of atomization particles. Identified was a variation law governing a decrease in average diameter span with an increase in outlet diameter. **Key words:** wet-process flue gas desulfurization, swirl nozzle, atomization characteristics

新型下排气旋风分离器的流场和性能数值模拟 = **Numerical Simulation of the Flow Field and Performance of an Innovative Cyclone Separator with a Downward Discharge of Gases** [刊, 汉] / HUANG Sheng-zhu (Department of Thermal Energy & Power Engineering, Harbin Institute of Technology, Weihai, Shandong Province, China, Post Code: 264209), ZHU Lin (Weihai Boiler Works, Weihai, Shandong Province, China, Post Code: 264200), MA Chun-yuan (Institute of Energy and Power Engineering under the Shandong University, Jinan, China, Post Code: 250061), WU Shao-hua (Department of Energy Science and Engineering, Harbin Institute of Technology, Harbin, China, Post Code: 150001) // Journal of Engineering for Thermal Energy & Power. — 2006, 21(1). — 70 ~ 74

By employing a RNG (Renormalization Group) $k-\epsilon$ turbulent flow model, RSM (Reynolds Stress model) turbulent flow model and a Lagrangian model in a CFD (computational fluid dynamics) software - Fluent a numerical simulation was carried out for the gas-phase flow field and separation efficiency of an innovative cyclone separator with a downward discharge of gases. The cyclone separator features an improved construction with its two sides cut at the inside and outside. An analysis of its specific features and separation performance shows that the gas flow of the cyclone separator has generated three branch flows, namely, an apex vortex ring flow, a flow characterized by a direct entry into an exhaust pipe, and a flow, which after rotating at the outer wall makes its way downward to come to a conic surface, and then turns back to flow upward. The composite vortex structure of a tangential velocity distribution appears to be not distinct. The graded efficiency and pressure losses at different outlet velocities, obtained by simulations, can be used as a practical reference during the engineering design and type selection of cyclone separators. **Key words:** cyclone separator, flow field, RNG (renormalization group) $k-\epsilon$ turbulent flow model, RSM (Reynolds stress model) turbulent model, numerical simulation

PEMFC 分布式发电系统动态协调控制仿真 = **Dynamic Simulation of Coordinated Control of PEMFC (Proton Exchange Membrane Fuel Cell) Distributed Power Generation System** [刊, 汉] / ZHANG Ying-ying, CAO Guang-yi, ZHU Xin-jian (Automation Department of Fuel Cell Research Institute under the Shanghai Jiaotong University, Shanghai, China, Post Code: 200030) // Journal of Engineering for Thermal Energy & Power. — 2006, 21(1). — 75 ~ 79, 95